

RESEARCH

Open Access



Optimal Mixture Design of Low-CO₂ High-Volume Slag Concrete Considering Climate Change and CO₂ Uptake

Han-Seung Lee¹, Seung-Min Lim² and Xiao-Yong Wang^{3*} 

Abstract

High-volume slag (HVS) can reduce the CO₂ emissions of concrete, but increase the carbonation depth of concrete. In particular, because of the effects of climate change, carbonation will accelerate. However, the uptake of CO₂ as a result of carbonation can mitigate the harm of CO₂ emissions. This study proposes an optimal mixture design method of low-CO₂ HVS concrete considering climate change, carbonation, and CO₂ uptake. Firstly, net CO₂ emissions are calculated by subtracting the CO₂ emitted by the material from the uptake of CO₂ by carbonation. The strength and depth of carbonation are evaluated by a comprehensive model based on hydration. Secondly, a genetic algorithm (GA) is used to find the optimal mixture. The objective function of the GA is net CO₂ emissions. The constraints of the GA include the strength, carbonation, workability, and range of concrete components. Thirdly, the results show that carbonation durability is a control factor of the mixture design of low-strength HVS concrete, while strength is a control factor of the mixture design of high-strength HVS concrete. After considering climate change, the threshold of strength control increases. With the increase of strength, the net CO₂ emissions increase, while the CO₂ uptake ratio decreases.

Keywords: mixture design, low-CO₂ concrete, high-volume slag, carbonation, CO₂ uptake, climate change

1 Introduction

Slag is a byproduct from iron- or steelmaking industry and is widely used to produce sustainable concrete. Use of slag can reduce the risk of alkali–aggregate reaction and enhance resistance to chloride ingress, sulfate attack, and other chemicals (Juenger and Siddique 2015). To achieve the aim of sustainability, high-volume slag (HVS) concrete, which contains about 70% slag in the binder, is increasingly used. Because HVS concrete has a lower carbonation resistance compared with control concrete, the carbonation durability of HVS concrete should be carefully considered (Rashad 2018; Lee and Wang 2016; Shah and Bishnoi 2018).

Many studies have evaluated the CO₂ emissions of concrete by incorporating mineral admixtures.

Robati et al. (2016) found that the application of supplementary cementitious materials can reduce CO₂ emissions by 16% compared with general practices. Zhang et al. (2019) proposed that concrete containing silica fume and fly ash shows superior environmental performance over plain concrete. Passuello et al. (2017) reported that the use of rice husk ash-derived sodium silicate can reduce the environment impact of geopolymer concrete by about 60%. Teh et al. (2017) determined greenhouse emissions of blended concrete based on process-based life cycle assessment and hybrid life cycle assessment. They found that hybrid life cycle assessment resulted in higher greenhouse emissions. Oliveira et al. (2016) estimated CO₂ life cycle emissions of concrete block manufacturers and found that cement consumption is the domain factor for CO₂ emissions. Kim et al. (2017) determined greenhouse gas emissions

*Correspondence: wxbrave@kangwon.ac.kr

³ Department of Architectural Engineering, Kangwon National University, Chuncheon-Si, South Korea

Full list of author information is available at the end of the article

Journal information: ISSN 1976-0485 / eISSN 2234-1315

for concrete with different strengths. They found that the raw material stage accounted for more than 90% of the greenhouse gas emissions.

Although many studies have been conducted to evaluate the CO₂ emissions of concrete, the number of studies on mixture designs of low-CO₂ concrete is relatively insufficient. Kim et al. (2016) proposed an evolution algorithm to produce concrete with minimum CO₂ emissions or cost. Based on the optimization method, 34% of CO₂ emissions can be reduced compared to the standard concrete production process. Park et al. (2013) used a genetic algorithm to design low-CO₂ concrete containing recycled concrete aggregate. The required properties of concrete, such as workability, strength, carbonation, and drying shrinkage, were considered (Park et al. 2013). Yang et al. (2015) determined the unit binder content and mineral admixture replacement level for a design strength and CO₂ reduction level. Based on a hybrid glow-worm swarm algorithm, Yepes et al. (2015) optimized the concrete road bridges in terms of CO₂ emissions. However, it should be recognized that methods in some references (Kim et al. 2016; Park et al. 2013; Yang et al. 2015; Yepes et al. 2015) show some weak points regarding the mixture design of HVS concrete. First, Kim et al. (2016), Yang et al. (2015), and Yepes et al. (2015) do not consider the constraint of carbonation of concrete. Because HVS concrete has a lower carbonation resistance, the requirement from carbonation durability should be carefully checked. Second, concrete can take up CO₂ due to carbonation (Kim and Chae 2016; Jang and Lee 2016; Fang et al. 2017; Possan et al. 2016). CO₂ uptake can alleviate the hazard of CO₂ emissions (Miller et al. 2018; Pacheco-Torgal et al. 2018). Previous studies do not consider the effect of CO₂ uptake on optimum mixture design. Third, due to climate change, CO₂ concentration and temperature increase, and thus the carbonation of concrete, will accelerate (Papadakis et al. 1991; Papadakis 2000; Demis et al. 2014). Previous studies do not consider the effect of climate change on optimum mixture design.

This study proposes a mixed design method of low-CO₂ HVS concrete that considers climate change, carbonation, and CO₂ uptake caused by carbonation. A genetic algorithm (GA) was used to determine the optimal mixture scheme. The objective function of the genetic algorithm is the net CO₂ emissions; that is, the CO₂ emissions of the concrete material minus the CO₂ uptake during carbonation. The comprehensive model of hydration–strength–carbonation was used to evaluate the performance of concrete. The influence of the design strength level and climate change scenario on the mixture design was evaluated.

2 Formulation for the Optimization of Concrete Mixing Proportions

In order to optimize the concrete mixture, objective function and constraint conditions should be established. This study takes net CO₂ emissions as the objective function. The net CO₂ emissions are equal to the CO₂ emissions of the material minus the CO₂ uptake caused by carbonation. Constraints include requirements on strength, durability, workability, component content, component ratio, and absolute volume (Yeh 2007).

2.1 Object Function

2.1.1 CO₂ Emissions of Concrete

The total CO₂ emissions of HVS concrete include the emissions of concrete materials, transportation, and mixing (Lee and Wang 2016). Total CO₂ emissions can be calculated as follows (Lee and Wang 2016):

$$CO_{2-e} = CO_{2-eM} + CO_{2-eT} + CO_{2-eP} \quad (1)$$

where CO_{2-e} , CO_{2-eM} , CO_{2-eT} , and CO_{2-eP} represent total CO₂ emissions, CO₂ emissions from concrete materials, CO₂ emissions from transport, and CO₂ emissions from the mixing operation of concrete, respectively. CO_{2-eM} can be calculated based on the concrete mixture and the unit CO₂ emissions of concrete components as follows:

$$CO_{2-eM} = CO_{2-C} * C + CO_{2-SG} * SG + CO_{2-W} * W + CO_{2-CA} * CA + CO_{2-S} * S + CO_{2-SP} * SP \quad (2)$$

where CO_{2-C} , CO_{2-SG} , CO_{2-W} , CO_{2-CA} , CO_{2-S} , and CO_{2-SP} are the unit CO₂ emissions of cement, slag, water, coarse aggregate, sand, and superplasticizer, respectively, and C , SG , W , CA , S , and SP are the mass of cement, slag, water, coarse aggregate, sand, and superplasticizer in concrete mixtures, respectively. Table 1 shows the CO₂ emissions of the concrete components (Yang et al. 2015).

2.1.2 CO₂ Uptake Due to Carbonation

CO₂ is absorbed by carbonation. The carbonation reaction of concrete can be described as follows (Papadakis 2000):

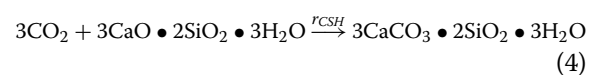


Table 1 CO₂ emissions of concrete components.

Water (kg/kg)	Cement (kg/kg)	Slag (kg/kg)	Sand (kg/kg)	Gravel (kg/kg)	Superplasticizer (kg/kg)
0.000,196	0.931	0.0265	0.0026	0.0075	0.25

According to Eqs. (3) and (4), 1 kg of calcium hydroxide (CH) and 1 kg of calcium silicate hydrate (CSH) can take up 0.594 kg of CO₂ and 0.385 kg of CO₂, respectively. Therefore, for 1 m³ of carbonated concrete, CO₂ uptake content $M = 0.594 CH + 0.385 CSH$, where CH and CSH represent the mass of CH and CSH in 1 m³ concrete, respectively.

For concrete structural units, CO₂ uptake is related to the exposed surface (S), carbonation depth (x_c), and CO₂ uptake content of 1 m³ of carbonated concrete (M) (Papadakis 2000). For example, consider a concrete column with a square section (length h_1 , area a_1 by a_1). The square column has four sides exposed to the surrounding environment; therefore, the exposure surface area is $S = 4 \times a_1 \times h_1$. In addition, the volume of the concrete column is $V = a_1 \times a_1 \times h_1$, and the exposed surface can be rewritten as $S = 4 V/a_1$. When the concrete volume is 1 m³, the exposed surface is $S = 4/a_1$. The CO₂ uptake content of concrete column (CO_{2UP}) can be determined as follows:

$$CO_{2UP} = M * S * x_c = (0.594CH + 0.385CSH) * (4/a_1) * x_c \tag{5}$$

According to Eq. (5), with the increase of surface-to-volume ratio ($4/a_1$), the uptake capacity of CO₂ increases. Equation (5) is valid for the concrete column. For other structural elements, such as slabs, we use a similar method to calculate the CO₂ uptake content. For example, consider a concrete slab in a building (the depth of the slab is h_2 and the area of the slab is $a_2 \times b_2$). The slab in the building has six surfaces, i.e. four lateral surfaces and two base surfaces. The four lateral surfaces of the slab are covered with wall elements so that the lateral surfaces are not accessible to environmental CO₂. Two base surfaces are accessible to environmental CO₂. The exposure surface area is $S_2 = 2 \times a_2 \times b_2$. In addition, the volume of concrete slab $V_2 = a_2 \times b_2 \times h_2$, and the exposed surface can be rewritten as $S_2 = 2 \times V_2/h_2$. When the concrete volume is 1 m³, the exposed surface is $S_2 = 2/h_2$. The CO₂ uptake content of the slab can be determined as follows:

$$CO_{2UP} = M * S * x_c = (0.594CH + 0.385CSH) * (2/h_2) * x_c \tag{6}$$

As shown in Eq. (6), as the surface-to-volume ratio $2/h_2$ increases, CO₂ uptake ability increases.

2.1.3 Object Function

This study takes net CO₂ emissions (CO_{2net}) as the objective function. The net CO₂ emissions equal the CO₂ emissions of the material minus the CO₂ uptake caused by carbonation. The optimization objective function is calculated as follows:

$$CO_{2net} = CO_{2-em} - CO_{2UP}. \tag{7}$$

2.2 Constraint Conditions

The objective function (minimum net CO₂ emissions) is subject to various constraints, such as concrete strength, durability, workability, component content, component ratio, and absolute volume (Yeh 2007).

Strength constraint means that the design strength should be higher than the required strength. The strength constraint formula is as follows:

$$f_c(t) \geq f_{cr}(t) \quad (t = 3, 7, 28 \dots \text{days}) \tag{8}$$

where $f_c(t)$ is the concrete strength at age t and $f_{cr}(t)$ is the required strength at age t .

HVS concrete has a lower carbonation resistance than plain concrete. Hence, for HVS concrete in an atmospheric environment, carbonation durability should be considered. The carbonation constraint of concrete is as follows:

$$x_c(t) \leq CV \quad (t = 30, 50, 100 \dots \text{years}) \tag{9}$$

where $x_c(t)$ is the carbonation depth at the exposure service life and CV is the cover depth of the concrete.

The workability constraint of fresh concrete is as follows:

$$Slump \geq Slump^r \tag{10}$$

where $Slump^r$ is the required slump of the concrete.

The range of component contents is as follows:

$$lower \leq component \leq upper \tag{11}$$

where the components are cement, slag, water, fine aggregate, coarse aggregate, or superplasticizer. Table 2 shows the lower and upper limits of the concrete components (Yeh 2007).

The component ratio constraint is as follows:

$$R_l \leq R_i \leq R_u \tag{12}$$

where R_i is the component ratio (water-to-binder, slag-to-binder, fine aggregate-to-total aggregate, total aggregate-to-binder, and water-to-solid ratios) and R_l and R_u are the lower and upper limits of the component ratio, respectively. Table 3 shows the component ratio constraints (Yeh 2007).

The absolute volume constraint is as follows:

$$\frac{W}{\rho_W} + \frac{C}{\rho_C} + \frac{SG}{\rho_{SG}} + \frac{S}{\rho_S} + \frac{CA}{\rho_{CA}} + \frac{SP}{\rho_{SP}} + V_{air} = 1 \tag{13}$$

Table 2 Lower and upper limits of concrete components.

	Cement (kg/m ³)	Slag (kg/m ³)	Water (kg/m ³)	Fine aggregate (kg/m ³)	Coarse aggregate (kg/m ³)
Lower	50	0	120	640	780
Upper	700	700	250	900	1050

Table 3 Component ratio constraints.

	Water-to-binder ratio	Slag-to-binder ratio	Fine aggregate-to-total aggregate ratio	Total aggregate-to-binder ratio	Water-to-solid ratio
Lower	0.2	0	0.4	2.0	0.08
Upper	0.75	0.70	0.52	6.4	0.12

where ρ_w , ρ_c , ρ_{SG} , ρ_s , ρ_{CA} , and ρ_{SP} are the densities of water, cement, slag, sand, coarse aggregate, and superplasticizer, respectively, and V_{air} is the volume of air in the concrete. The densities of water, cement, slag, sand, coarse aggregate, and superplasticizer are 1000, 3150, 2890, 2610, 2700, and 1220 kg/m³, respectively. Equation (13) means that the sum of each concrete component should equal 1 m³ (Yeh 2007).

2.3 Property Evaluation of Slag-Blended Concrete

In our previous research (Lee and Wang 2016; Wang and Park 2017), we proposed a comprehensive model of HVS concrete hydration, strength, and durability. The reaction level of cement and slag is calculated according to a blended cement hydration model. According to the reaction degree of the binder, the compressive strength and carbonatable substance content of the binder were calculated. The carbonation depth of HVS concrete was predicted according to its properties and exposure conditions. The input parameters of the hydration–strength–durability model are the concrete mixture and curing conditions. The output of the comprehensive model is the performance of concrete, such as thermal performance, mechanical performance, and durability performance. The comprehensive model is applicable to concrete with different strength grades (high, medium, and low strength) and different slag substitution grades (low and high slag content) (Lee and Wang 2016; Wang and Park 2017).

2.3.1 Strength Development Model

The compressive strength of slag-blended concrete f_c can be analyzed based on the contents of calcium silicate hydrate as follows (Lee and Wang 2016; Wang and Park 2017):

$$CSH(t) = 2.85(f_{S,C} * C * \alpha + f_{S,P} * SG * \alpha_{SG}) \quad (14)$$

$$f_c(t) = 57.41 \frac{CSH(t)}{W} - 11.63 \quad (15)$$

where α and α_{SG} are the reaction degrees of cement and slag, respectively, and $f_{S,C}$ and $f_{S,P}$ are the weight fractions of SiO₂ in cement and slag, respectively. The

coefficient 2.85 is the ratio between the molar weight of CSH and the weight of the oxide SiO₂ in CSH. The reaction degree of cement α can be determined using the integral method in the time domain ($\alpha = \int_0^t \frac{d\alpha}{dt}$, where $\frac{d\alpha}{dt}$ is the reaction rate of cement). Similarly, the reaction degree of slag can be determined as $\alpha_{SG} = \int_0^t \frac{d\alpha_{SG}}{dt}$, where $\frac{d\alpha_{SG}}{dt}$ is the reaction rate of slag. The detailed equations for $\frac{d\alpha}{dt}$ and $\frac{d\alpha_{SG}}{dt}$ are available in our previous studies (Lee and Wang 2016; Wang and Park 2017). The unit of compressive strength in Eq. (15) is MPa.

The validations of hydration model and strength model are shown in Fig. 1a, b, respectively. For the test of the reaction degree of slag, the water-to-binder ratio of paste specimens was 0.5, the replacement level of slag was between 0 and 67%, and curing temperature varied from 5 to 40 °C. For the strength test, the water-to-binder ratio was 0.59, the slag substitution ratio was 0–0.75, the ages in the compressive strength test were 1 day–18 months, and the curing temperature was 20 °C.

Figure 1c–f shows the parameter analysis of reaction degree and strength development of slag-blended concrete. When slag replaces a proportion of the cement, the degree of hydration of cement increases due to the dilution effect of slag (Fig. 1c). For concrete with a low water-to-binder ratio, the dilution effect is very important, and the degree of hydration of cement increases more significantly (Fig. 1c). With the increase of slag substitution rate, the alkaline activation effect of calcium hydroxide becomes weaker and the reaction amount of slag also decreases (Fig. 1d). For concrete with a low water-to-binder ratio, the increment of compressive strength is more obvious than for concrete with a high water-to-binder ratio (Fig. 1e, f). For concrete with a low water-to-binder ratio, the dilution effect of slag is obvious.

2.3.2 Carbonation Model

When relative humidity is higher than 50%, there is a carbonation front which distinguishes the carbonation and noncarbonation zones of concrete. The carbonation depth of slag-blended concrete can be analyzed as follows (Lee and Wang 2016; Papadakis 2000):

$$x_c = \sqrt{\frac{2D[CO_2]_0t}{[CH] + 3[CSH]}} \quad (16)$$

$$D = 6.1 * 10^{-6} \left(\frac{\varepsilon}{\frac{C}{\rho_C} + \frac{W}{\rho_w} + \frac{SG}{\rho_{SG}}} \right)^3 \left(1 - \frac{RH}{100} \right)^{2.2} \quad (17)$$

where x_c is the carbonation depth of concrete, D is the CO₂ diffusivity, $[CO_2]_0$ is the CO₂ molar concentration at the concrete surface, $[CH]$ is the molar content of calcium

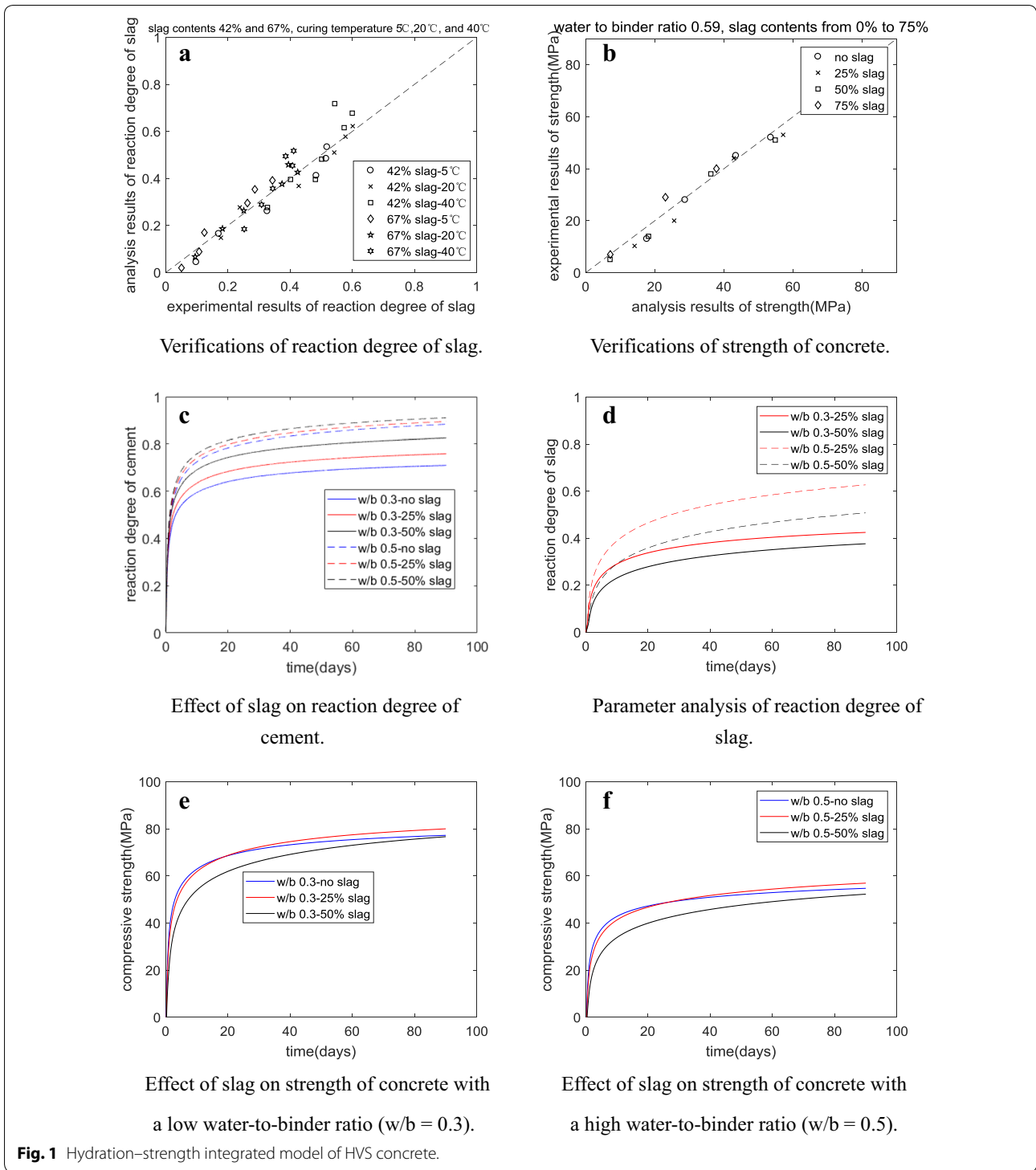


Fig. 1 Hydration–strength integrated model of HVS concrete.

hydroxide, $[CSH]$ is the molar content of CSH produced, ε is the concrete porosity, and RH is the environmental relative humidity. $[CH] + 3[CSH]$ in the denominator of Eq. (16) is the content of carbonatable material. For climate change conditions, CO_2 concentration and

diffusivity are dependent on time. The time-averaged CO_2 concentration $\frac{\int_0^t [CO_2]_t dt}{t}$ and CO_2 diffusivity $\frac{\int_0^t [D]_t dt}{t}$ were used for climate change conditions (Lee and Wang 2016; Papadakis 2000).

The calcium content in Eq. (16) can be determined using the binders' reaction degree as follows:

$$CH = C * \alpha * CH_{CE} - SG * \alpha_{SG} * \nu_{SG} \tag{18}$$

where CH_{CE} is the content of produced calcium hydroxide when the unit of cement becomes hydrated and ν_{SG} is the content of the consumed calcium hydroxide when the unit of slag reacts. Equation (18) considers both calcium hydroxide production from cement hydration and calcium hydroxide consumption from the slag reaction.

The porosity of concrete ε can be determined using the binders' reaction degree as follows:

$$\varepsilon = W / \rho_W - 0.25 * C * \alpha - 0.3 * \alpha_{SG} * SG - \Delta\varepsilon_C \tag{19}$$

where $\Delta\varepsilon_C$ is the porosity reduction due to carbonation, which can be determined based on the volumetric variation of the reactants and reaction products of carbonation (Lee and Wang 2016; Papadakis 2000).

The effects of environmental temperature on CO_2 diffusivity can be considered using the Arrhenius equation as follows:

$$D(T) = D_{ref} \exp \left[\beta \left(\frac{1}{T_{ref}} - \frac{1}{T} \right) \right] \tag{20}$$

where D_{ref} is the CO_2 diffusivity at reference temperature T_{ref} , $D(T)$ is the CO_2 diffusivity at temperature T , and β is the activation energy of CO_2 ($\beta = 4000$) (Stewart et al. 2011).

Figure 2a shows the verification of carbonation model (water-to-binder ratio of specimen was 0.59, slag-substitution ratio was 0–0.75, and curing age before

carbonation test was 3 days or 28 days). Figure 2b shows the parameter analysis of carbonation of slag-blended concrete. When slag replaces a proportion of the cement, the carbonation depth of concrete increases. The carbonation depth decreases with the decrease of the water-to-binder ratio.

2.3.3 Workability Model

According to previous experimental results (Lim et al. 2004; Thomas 2013), the slump of slag-blended concrete can be determined by the following:

$$\begin{aligned} slump = & -250 * \frac{W}{C + SG} + 0.088 * W - 146 \frac{S}{S + CA} \\ & + 18 * \frac{SG}{C + SG} + 0.199 * SP + 341. \end{aligned} \tag{21}$$

This equation implies that concrete slump increases with water content, slag substitution ratio, and superplasticizer content and reduces with the water-to-binder ratio and sand ratio. The unit of measurement in Eq. (21) is mm.

According to the mixing proportions of Lim et al. (2004), the relation between superplasticizer content and water-to-binder ratio is shown as follows:

$$\begin{aligned} SP = & 18.43 - 37.11 \frac{W}{C + SG} \quad (\text{for } \frac{W}{C + SG} \leq 0.5) \\ SP = & 0 \quad (\text{for } \frac{W}{C + SG} > 0.5) \end{aligned} \tag{22}$$

This equation implies that once the water-to-binder ratio decreases, the superplasticizer content in the concrete mixtures should increase. Additionally, it should

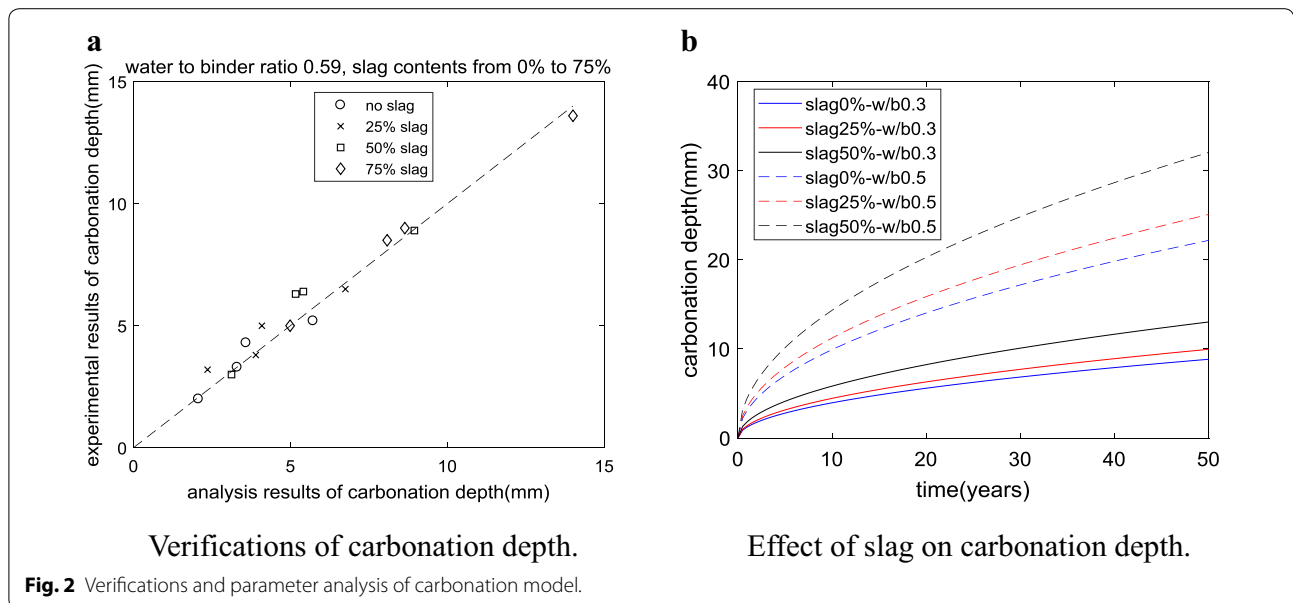
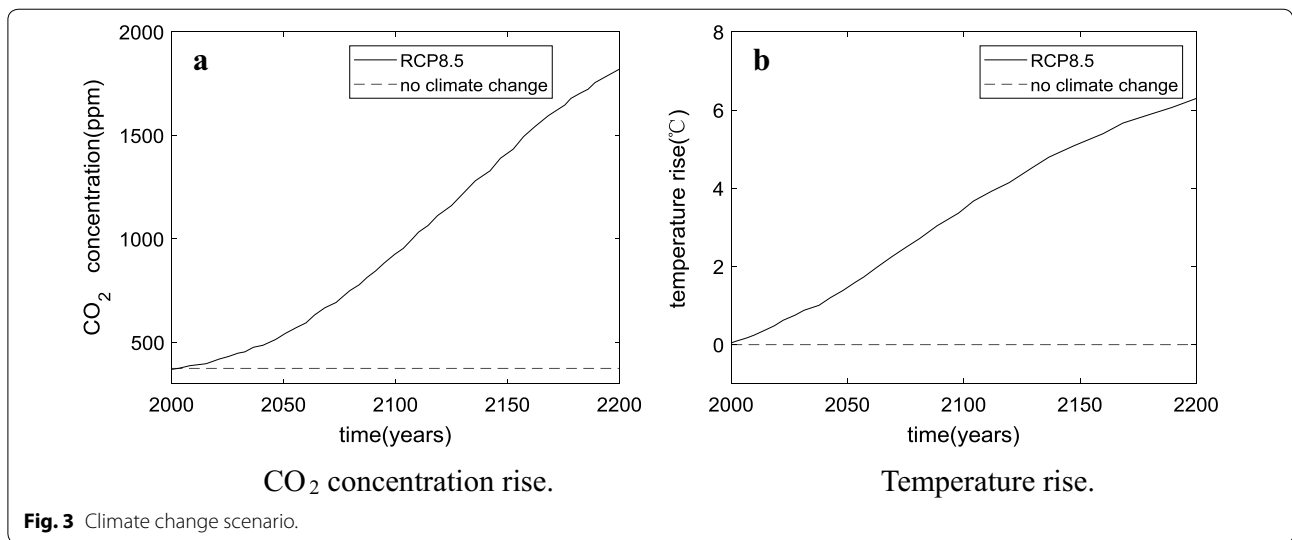


Fig. 2 Verifications and parameter analysis of carbonation model.



be noted that Eqs. (21) and (22) are regressed from references (Lim et al. 2004; Thomas 2013). If the brands of superplasticizer are altered, the equation might be different.

2.3.4 Summary of Property Evaluation Model

In the second section, we determine the constraint conditions and the objective function of concrete mixture optimization. We set the objective function as the minimum net CO₂ emissions. These constraint conditions include properties such as strength, carbonation durability, and workability. The strength and carbonation of HVS concrete were evaluated by the blended cement hydration model proved by our previous studies (Lee and Wang 2016; Wang and Park 2017). Once the objective function and constraint conditions are solved, concrete mixtures satisfying various performance parameters can be obtained.

The technique of solving the objective function with constraints involves the genetic algorithm (Mathworks 2019). The genetic algorithm originates from the computer simulation of biological systems. The basic steps of the genetic algorithm are: (1) generate a random population; (2) determine the individual fitness and make selections according to the fitness; (3) generate new individuals based on crossover and mutation operations; (iv) check termination conditions. If the termination condition is not met, return to step (2).

In this study, we used the MATLAB global optimization toolbox to optimize the target with constraint conditions (Mathworks 2019). The objective function and constraint equation were set in the MATLAB global optimization toolbox, and the optimal mixture satisfying

various constraints was found according to the genetic algorithm.

3 Illustrations of Design Examples

We designed low-CO₂ HVS concrete under different strengths and climate change scenarios. The design strengths are 25, 35, 45, and 55 MPa. The climate change scenario includes two levels: the RCP 8.5 climate change scenario and no climate change scenario. RCP 8.5 was proposed by the Intergovernmental Panel on Climate Change (IPCC) (Pachauri and Meyer 2014). As shown in Fig. 3, the RCP 8.5 scenario considers the increment of CO₂ concentration and temperature. Eight hybrid conditions were calculated by combining four design strengths with two climate change scenarios. The design structural unit is a concrete column with a section of 500 × 500 mm.

The exposure conditions were assumed to be temperate (see Table 4). The required strength of concrete in temperate climate is 25 MPa, concrete cover depth is 30 mm, and the average exposure temperature is 15 °C (Stewart et al. 2011). The required service life of concrete is 50 years. The air content of concrete, V_{air} , is assumed to be 2%. The required slump of concrete is 170 mm. Assuming that the relative humidity is 0.7, the

Table 4 Summary of exposure conditions.

	Designed compressive strength (MPa)	Cover depth (mm)	Average temperature (°C)	Relative humidity
Temperate climate	25	30	15	0.7

concrete begins to carbonate after 28 days of curing. The initial time of carbonation exposure was the year 2000.

3.1 Mixture Design without Climate Change

In this section, we designed concretes of different strength without considering climate change. The concrete mixtures were determined based on the genetic algorithm considering the objective function and various constraints. As shown in Table 5, Mix1, Mix2, Mix3, and Mix4 correspond to the design strengths of 25 MPa, 35 MPa, 45 MPa, and 55 MPa, respectively. Table 5 shows that the water content of concrete with different strengths is similar. This is because the lower bound of the water-to-solid ratio is 0.08. The slag replacement ratio of each mixture is the same. This is because the upper limit of slag-to-binder ratio is 0.7. In addition, we found that the content of binder increased with the increase of concrete strength. We also found that the mixing proportion of Mix1 is the same as Mix2, although Mix2 (35 MPa) has a higher design strength than Mix1 (25 MPa). This is because for low-strength HVS concrete, carbonation durability is the dominant factor in mixture design.

The design strength, real strength, slump, carbonation depth after 50 years' service life, CO₂ emission, and CO₂ uptake after 50 years' service life are shown in Table 6. According to Table 6, the real strength of Mix1 and Mix2

is 35.45 MPa, which is higher than the design strength of Mix1 (25 MPa) and Mix2 (35 MPa). In other words, for HVS concrete, the strength of 25 and 35 MPa is not enough to meet the requirement of carbonation durability, and the minimum strength to meet the requirement of carbonation durability is 35.45 MPa. In addition, for Mix3 (45 MPa) and Mix4 (55 MPa), the design strength is equal to the real strength. This is because, for high-strength HVS concrete, concrete strength is the dominant factor. In summary, for HVS concrete, when the design strength is lower than 35.45 MPa, carbonation is the dominant factor in the mixture design. When the design strength is greater than 35.45 MPa, the strength is the dominant factor in the mixture design.

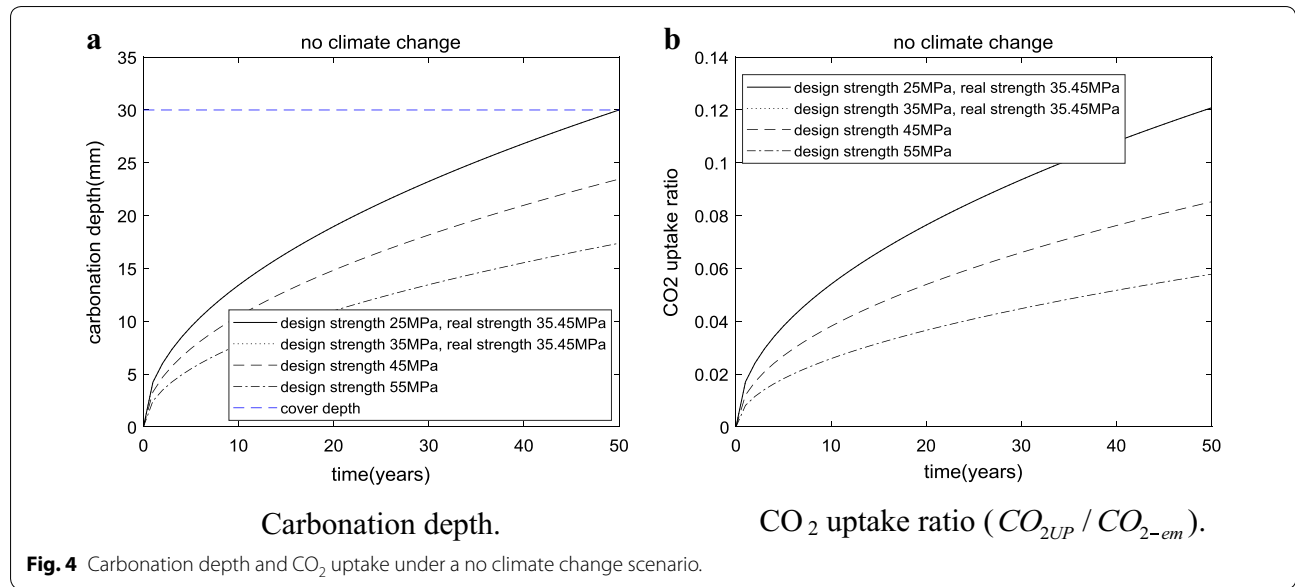
Figure 4a shows the carbonation depth of concrete with different mixtures. For Mix1 or Mix2, 50 years later, the carbonation depth is equal to the cover depth of 30 mm. For Mix3 and Mix4, the carbonation depth is less than 30 mm. With the increase of concrete strength, concrete carbonation depth decreases. Figure 4b shows the CO₂ uptake ratios CO_{2LUP}/CO_{2-em} (the ratio of CO₂ uptake to CO₂ emission). We found that CO₂ uptake ratios decreased with the increase of concrete strength. This is because with the increase of concrete strength, CO₂ emission increases and CO₂ uptake decreases (Table 6). The CO₂ uptake content relates to the carbonation depth and the content of carbonatable substance. With the increase of concrete strength, the contents of binder and

Table 5 Mixtures of concrete under a no climate change scenario.

No climate change	Water (kg/m ³)	Cement (kg/m ³)	Slag (kg/m ³)	Fine aggregate (kg/m ³)	Coarse aggregate (kg/m ³)	Superplasticizer (kg/m ³)
Mix1: design strength of 25 MPa	174.06	110.21	257.16	900.00	908.40	0.85
Mix2: design strength of 35 MPa	174.06	110.21	257.16	900.00	908.40	0.85
Mix3: design strength of 45 MPa	174.09	136.42	318.31	895.14	826.28	4.22
Mix4: design strength of 55 MPa	174.48	170.05	396.78	834.18	780.00	7.01

Table 6 Performance of concrete under a no climate change scenario.

No climate change	Design strength (MPa)	Real strength (MPa)	Slump (mm)	Carbonation depth (mm)	CO ₂ emissions from materials (kg/m ³)	CO ₂ uptake (kg/m ³)	Net CO ₂ emissions (kg/m ³)	CO ₂ uptake ratio
Mix1: design strength of 25 MPa	25.00	35.45	177.73	30.00	118.82	14.36	104.46	0.121
Mix2: design strength of 35 MPa	35.00	35.45	177.73	30.00	118.82	14.36	104.46	0.121
Mix3: design strength of 45 MPa	45.00	45.00	197.96	23.46	145.05	12.37	132.69	0.085
Mix4: design strength of 55 MPa	55.00	55.00	217.84	17.39	178.63	10.33	168.30	0.058



carbon substance (CH and CSH) increased. This factor will increase the uptake capacity of CO₂. However, as the strength of concrete increases, the carbonation depth decreases. This factor reduces the uptake of CO₂. Since the reduced factor is more significant than the increased factor, the increasing of strength reduces CO₂ uptake content.

3.2 Mixture Design with Climate Change

Section 3.1 does not consider the impact of climate change on mixture design. In this section, we describe the design of low-CO₂ HVS concrete considering the impact of climate change. Assuming the climate change scenario is RCP 8.5 (Fig. 3), mixtures with different strength grades are calculated based on the genetic algorithm considering the objective function and constraints. The design strengths of Mix5, Mix6, Mix7, and Mix8 are 25, 35, 45 and 55 MPa, respectively (shown in Table 7). We discovered that Mix5 is the same as Mix6 (in this case, like Mix1 and Mix2). This is because for low-strength HVS concrete (Mix5 and Mix6), carbonation durability is the dominant factor in mixture design. On the other

hand, we found that the binder content of Mix5 and Mix6 was higher than that of Mix1 and Mix2. The increase of binder content can increase the content of carbonatable substances, lower the porosity, and increase carbonation resistance. For low-strength HVS concrete, in order to meet the requirements of climate change on carbonation durability, a higher binder content is required. Furthermore, we find that for high-strength concrete (45 MPa and 55 MPa), climate change does not change the concrete mixtures (Mix3 and Mix4 are the same as Mix7 and Mix8, respectively).

Table 8 shows the performance of HVS concrete when considering climate change. The real strength of Mix6 and Mix7 is 39.55 MPa, higher than that of Mix1 and Mix2 (35.45 MPa). This means that for low-strength HVS concrete, design strength needs to be increased in order to mitigate the challenges of climate change. In addition, climate change does not affect the mix design of high-strength HVS concrete (Mix7 and Mix8).

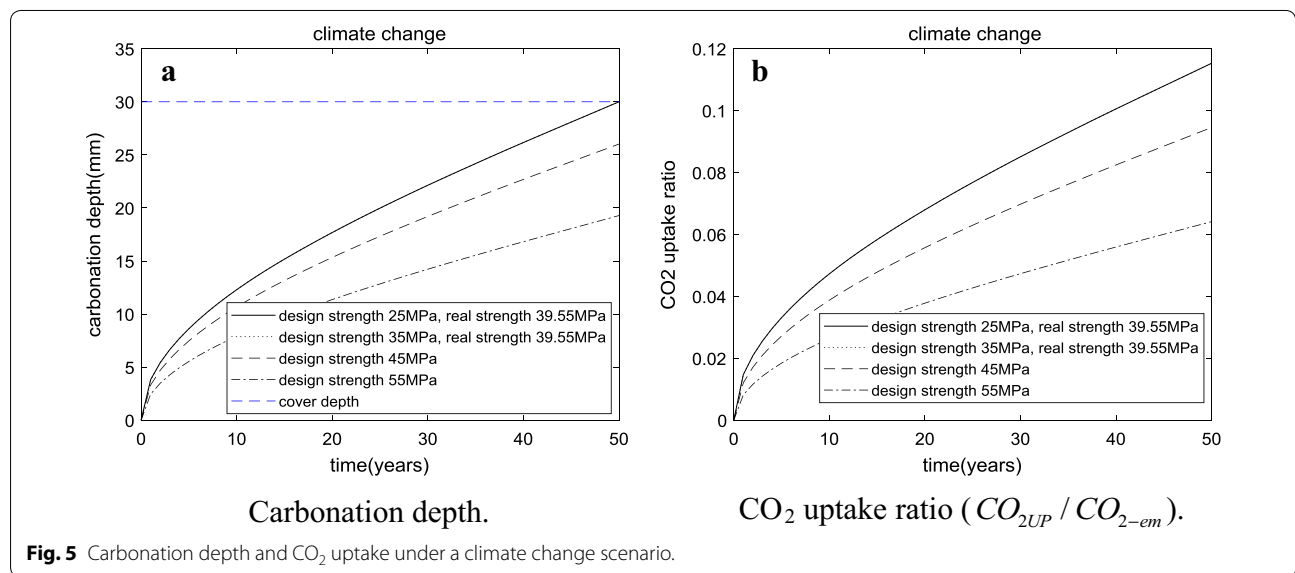
Figure 5a shows the carbonation depth of concrete under the climate change scenario of RCP 8.5. Fifty years later, Mix5 and Mix6 are carbonated to the same depth

Table 7 Mixtures of concrete under a climate change scenario.

Climate change	Water (kg/m ³)	Cement (kg/m ³)	Slag (kg/m ³)	Fine aggregate (kg/m ³)	Coarse aggregate (kg/m ³)	Superplasticizer (kg/m ³)
Mix5: design strength of 25 MPa	174.04	121.04	282.43	900.00	872.07	2.42
Mix6: design strength of 35 MPa	174.04	121.04	282.43	900.00	872.07	2.42
Mix7: design strength of 45 MPa	174.09	136.42	318.31	895.14	826.28	4.22
Mix8: design strength of 55 MPa	174.48	170.05	396.78	834.18	780.00	7.01

Table 8 Performance of concrete under a climate change scenario.

Climate change	Design strength (MPa)	Real strength (MPa)	Slump (mm)	Carbonation depth (mm)	CO ₂ emissions from materials (kg/m ³)	CO ₂ uptake (kg/m ³)	Net CO ₂ emissions (kg/m ³)	CO ₂ uptake ratio
Mix5: design strength of 25 MPa	25.00	39.55	187.20	30.00	129.70	14.95	114.74	0.115
Mix6: design strength of 35 MPa	35.00	39.55	187.20	30.00	129.70	14.95	114.74	0.115
Mix7: design strength of 45 MPa	45.00	45.00	197.96	26.02	145.05	13.72	131.34	0.095
Mix8: design strength of 55 MPa	55.00	55.00	217.84	19.28	178.63	11.46	167.17	0.064



as their 30 mm cover depth. This is because carbonation durability dominates the mixture design of low-strength HVS concrete. By comparing Figs. 4a and 5a, we find that climate change has accelerated carbonation (the carbonation depth of Mix7 and Mix8 is higher than that of Mix3 and Mix4, respectively). Figure 5b shows the CO₂ uptake ratio. With the increase of strength, CO₂ uptake ratio decreases.

Figure 6a shows the CO₂ uptake content after a service life of 50 years. It shows that when the compressive strength is the same, climate change will increase the content of CO₂ taken up. This is due to an increase in carbonation depth. Figure 6b shows when the compressive strength is the same, climate change increases CO₂ uptake ratios. Figure 6c shows as concrete strength increases, net CO₂ emissions increase. When the compressive strength is the same, climate change slightly lowers the net CO₂ emissions of concrete.

3.3 Effect of Structural Elements on Mixture Design and CO₂ Uptake

In Sects. 3.1 and 3.2, structural units are assumed to be concrete columns with a cross section of 500 × 500 mm². In this section, we discuss the effects of structural element types on optimal mixtures and CO₂ uptake.

First, the structural unit is assumed to be a slab (with a depth of 180 mm and a design strength of 55 MPa, considering climate change). Based on the genetic algorithm, the same optimal mixture as that of Mix8 is obtained. In other words, changes in the type of structural units do not affect the optimal concrete mix. However, as shown in Fig. 7a, the CO₂ uptake ratio of the slab is higher than that of the column (this is because the surface area-to-volume ratio of the slab is higher than that of the column).

Secondly, the slab thickness was changed from 160 to 200 mm (combined with climate change, the design

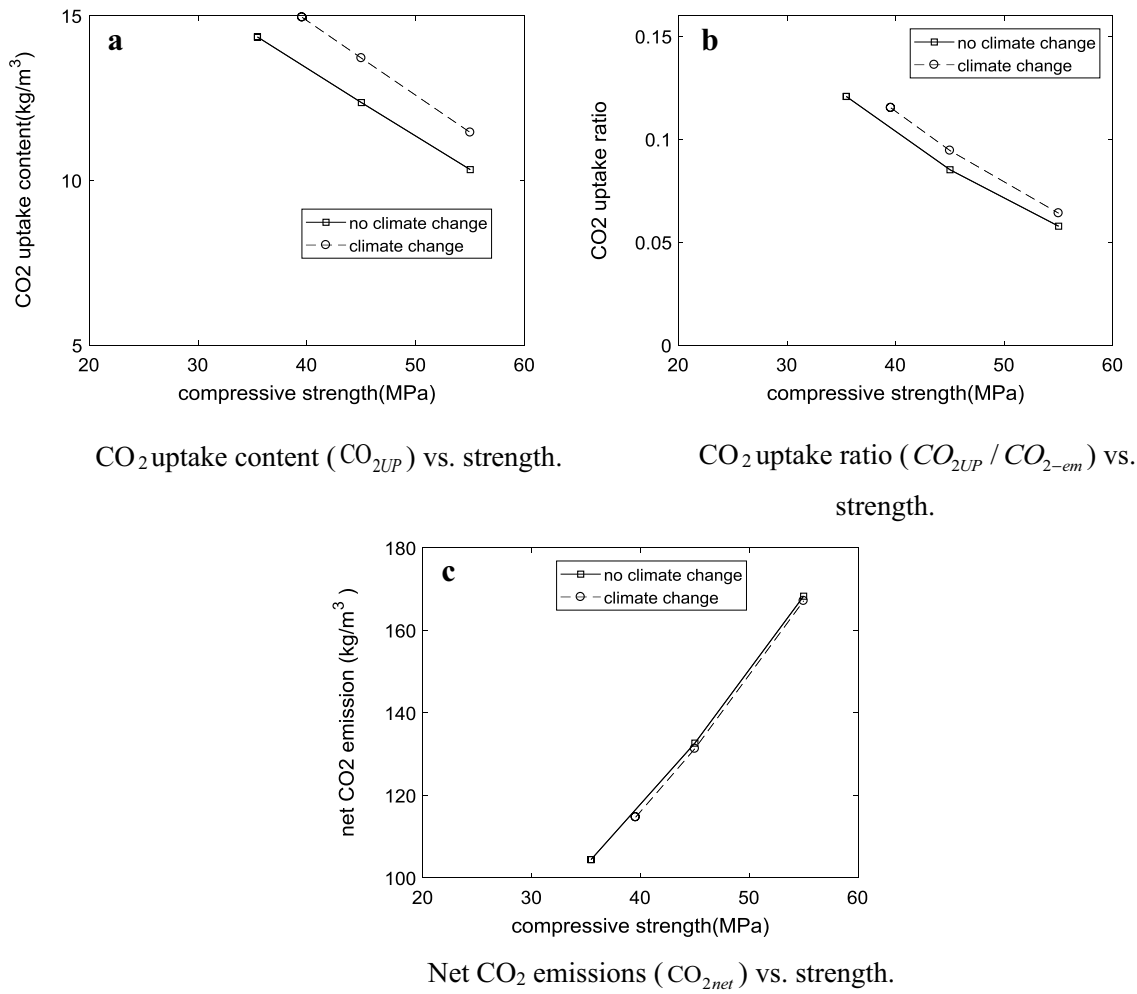


Fig. 6 Effect of strength on CO₂ uptake content (CO_{2UP}), CO₂ uptake ratio (CO_{2UP}/CO_{2-em}), and net CO₂ emissions (CO_{2net}).

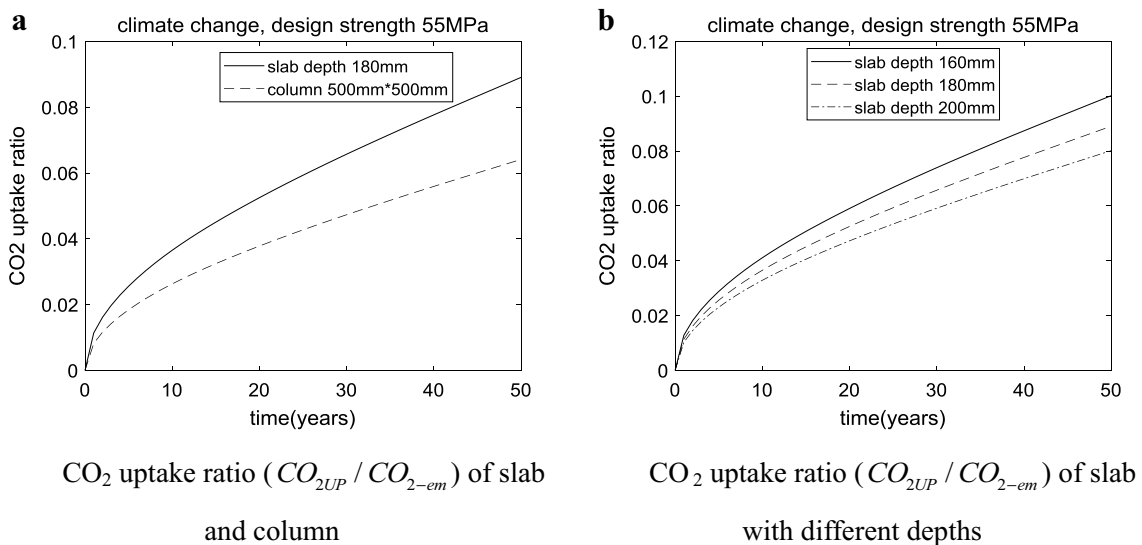


Fig. 7 Effect of structural element types on CO₂ uptake ratio (CO_{2UP}/CO_{2-em}).

strength was 55 MPa). Based on the genetic algorithm, the same optimal mixture as that of Mix8 is obtained. In other words, changes in slab thickness do not affect the optimal concrete mix. As the slab depth decreases, its surface volume ratio and CO₂ uptake ratio increase (as shown in Fig. 7b).

Based on the analysis of these parameters, we found that the optimal mixture of low-CO₂ HVS concrete did not change with the change of type and size of structural units. However, the CO₂ uptake increases with the increase of the surface area-to-volume ratio.

4 Conclusions

In this study, a genetic algorithm was proposed to optimize the design of low-CO₂ HVS concrete mixture considering climate change, carbonation, and CO₂ uptake.

First, the objective function of the genetic algorithm is the net CO₂ emissions; that is, the material CO₂ emissions minus the CO₂ uptake. The uptake of CO₂ is determined by the depth of carbonation, carbonatable substances content, and the geometry of structural elements. The constraints of the genetic algorithm include the strength, carbonation durability, workability, and range of concrete components. Based on the hydration model, the strength and carbonation depth were evaluated.

Secondly, the optimal mixtures under different strength levels and climate change scenarios were determined. Carbonation durability dominates the mixture design of low-strength HVS concrete, while compressive strength dominates the mixture design of high-strength HVS. Under the conditions of no climate change and climate change, respectively, the strength control threshold is 35.45 MPa and 39.55 MPa. For low-strength HVS concrete, a rich mix of materials must be used in order to mitigate the hazards of climate change.

Third, with the increase of strength, the net emissions of CO₂ also increase and CO₂ uptake ratio decreases. When compressive strength is the same, climate change will increase CO₂ uptake content. With the change of structural element type and size, the optimal mixture of low-CO₂ HVS concrete does not change. With the increase of surface area-to-volume ratio, the CO₂ uptake ratio increases.

Fourth, other researchers could substitute their own equations for those for CO₂ emissions, compressive strength, carbonation depth, and slump. In this way, using a genetic algorithm, low-CO₂ HVS concrete can be designed to meet the domestic requirements. The method presented in this paper is a general method for considering both sustainability and durability.

Acknowledgements

This research was supported by the Basic Science Research Program through the National Research Foundation of Korea (NRF) funded by the Ministry of Science, ICT & Future Planning (No. 2015R1A5A1037548), and an NRF Grant (NRF-2017R1C1B1010076).

Authors' contributions

Data curation, HSL, SML, and XYW; Formal analysis, SML and XYW; Methodology, HSL, SML, and XYW; Supervision, HSL, and XYW; writing—original draft, HSL, SML, and XYW. All authors read and approved the final manuscript.

Funding

Funder: National Research Foundation of Korea. Award number: NRF-2015R1A5A1037548 and NRF-2017R1C1B1010076.

Availability of data and materials

The datasets used and/or analyzed during the current study are available from the corresponding author on reasonable request.

Competing interests

I confirmed that I have read Springer Open's guidance on competing interests and have included a statement indicating that none of the authors have any competing interests in the manuscript.

Author details

¹ Department of Architectural Engineering, Hanyang University, Ansan-Si, Korea. ² Department of Architecture, Kangwon National University, Chuncheon-Si, Korea. ³ Department of Architectural Engineering, Kangwon National University, Chuncheon-Si, South Korea.

Received: 22 March 2019 Accepted: 11 July 2019

Published online: 16 September 2019

References

- Demis, S., Efstathiou, M. P., & Papadakis, V. G. (2014). Computer-aided modeling of concrete service life. *Cement & Concrete Composites*, 47, 9–18. <https://doi.org/10.1016/j.cemconcomp.2013.11.004>.
- Fang, X. L., Xuan, D. X., & Poon, C. S. (2017). Empirical modelling of CO₂ uptake by recycled concrete aggregates under accelerated carbonation conditions. *Materials and Structures*, 50, 200–213. <https://doi.org/10.1617/s11527-017-1066-y>.
- Jang, J. G., & Lee, H. K. (2016). Microstructural densification and CO₂ uptake promoted by the carbonation curing of belite-rich Portland cement. *Cement and Concrete Research*, 82, 50–57. <https://doi.org/10.1016/j.cemconres.2016.01.001>.
- Juenger, M. C., & Siddique, R. (2015). Recent advances in understanding the role of supplementary cementitious materials in concrete. *Cement and Concrete Research*, 78, 71–80. <https://doi.org/10.1016/j.cemconres.2015.03.018>.
- Kim, T. H., & Chae, C. U. (2016). Evaluation analysis of the CO₂ emission and uptake life cycle for precast concrete in Korea. *Sustainability*, 8, 663–676. <https://doi.org/10.3390/su8070663>.
- Kim, T. H., Lee, S. H., Chae, C. U., Jang, H. J., & Lee, K. H. (2017). Development of the CO₂ emission evaluation tool for the life cycle assessment of concrete. *Sustainability*, 9, 2116–2130. <https://doi.org/10.3390/su9112116>.
- Kim, T. H., Tae, S. H., Suk, S. J., Ford, G., & Yang, K. H. (2016). An optimization system for concrete life cycle cost and related CO₂ emissions. *Sustainability*, 8, 361–380. <https://doi.org/10.3390/su8040361>.
- Lee, H. S., & Wang, X. Y. (2016). Evaluation of compressive strength development and carbonation depth of high volume slag-blended concrete. *Construction and Building Materials*, 124, 45–54. <https://doi.org/10.1016/j.conbuildmat.2016.07.070>.
- Lim, C. H., Yoon, Y. S., & Kim, J. H. (2004). Genetic algorithm in mix proportioning of high-performance concrete. *Cement and Concrete Research*, 34, 409–420. <https://doi.org/10.1016/j.cemconres.2003.08.018>.
- Mathworks (2019) <http://www.mathworks.com>. Accessed 1 Jan 2019.

- Miller, S. A., John, V. M., Pacca, S. A., & Horvath, A. (2018). Carbon dioxide reduction potential in the global cement industry by 2050. *Cement and Concrete Research*, 114, 115–124. <https://doi.org/10.1016/j.cemconres.2017.08.026>.
- Oliveira, L. S., Pacca, S. A., & John, V. M. (2016). Variability in the life cycle of concrete block CO₂ emissions and cumulative energy demand in the Brazilian Market. *Construction and Building Materials*, 114, 588–594. <https://doi.org/10.1016/j.conbuildmat.2016.03.134>.
- Pachauri, P. K., Meyer, L. A. (2014). *IPCC: climate change 2014: synthesis report*. Contribution of working groups I, II and III to the fifth assessment report of the intergovernmental panel on climate change [Core Writing Team, (eds.)]. IPCC, Geneva, Switzerland, pp 151.
- Pacheco-Torgal, F., Shi, C., & Palomo, A. (Eds.). (2018). *Carbon dioxide sequestration in cementitious construction materials*. Cambridge: Woodhead Publishing.
- Papadakis, V. G. (2000). Effect of supplementary cementing materials on concrete resistance against carbonation and chloride ingress. *Cement and Concrete Research*, 30, 291–299. [https://doi.org/10.1016/S0008-8846\(99\)00249-5](https://doi.org/10.1016/S0008-8846(99)00249-5).
- Papadakis, V. G., Vayenas, C. G., & Fardis, M. N. (1991). Fundamental modeling and experimental investigation of concrete carbonation. *ACI Materials Journal*, 88, 363–373.
- Park, W. J., Noguchi, T., & Lee, H. S. (2013). Genetic algorithm in mix proportion design of recycled aggregate concrete. *Computers and Concrete*, 11, 183–199. <https://doi.org/10.12989/cac.2013.11.3.183>.
- Passuello, A., Rodríguez, E. D., Hirt, E., Longhi, M., Bernal, S. A., Provis, J. L., et al. (2017). Evaluation of the potential improvement in the environmental footprint of geopolymers using waste-derived activators. *Journal of Cleaner Production*, 166, 680–689. <https://doi.org/10.1016/j.jclepro.2017.08.007>.
- Possan, E., Felix, E. F., & Thomaz, W. A. (2016). CO₂ uptake by carbonation of concrete during life cycle of building structures. *Journal of Building Pathology and Rehabilitation*, 1, 1–9. <https://doi.org/10.1007/s41024-016-0010-9>.
- Rashad, A. M. (2018). An overview on rheology, mechanical properties and durability of high volume slag used as a cement replacement in paste, mortar and concrete. *Construction and Building Materials*, 187, 89–117. <https://doi.org/10.1016/j.conbuildmat.2018.07.150>.
- Robati, M., Carthy, T. J. M., & Kokogiannakis, G. (2016). Incorporating environmental evaluation and thermal properties of concrete mix designs. *Construction and Building Materials*, 128, 422–435. <https://doi.org/10.1016/j.conbuildmat.2016.10.092>.
- Shah, V., & Bishnoi, S. (2018). Carbonation resistance of cements containing supplementary cementitious materials and its relation to various parameters of concrete. *Construction and Building Materials*, 178, 219–232. <https://doi.org/10.1016/j.conbuildmat.2018.05.162>.
- Stewart, M. G., Wang, X. M., & Nguyen, M. N. (2011). Climate change impact and risks of concrete infrastructure deterioration. *Engineering Structures*, 33, 1326–1337. <https://doi.org/10.1016/j.engstruct.2011.01.010>.
- Teh, S. H., Wiedmann, T., Castel, A., & de Burgh, J. (2017). Hybrid life cycle assessment of greenhouse gas emissions from cement, concrete and geopolymer concrete in Australia. *Journal of Cleaner Production*, 152, 312–320. <https://doi.org/10.1016/j.jclepro.2017.03.122>.
- Thomas, M. (2013). *Supplementary cementing materials in concrete*. New York: CRC press, Taylor & Francis Group.
- Wang, X. Y., & Park, K. B. (2017). Analysis of the compressive strength development of concrete considering the interactions between hydration and drying. *Cement and Concrete Research*, 102, 1–15. <https://doi.org/10.1016/j.cemconres.2017.08.010>.
- Yang, K. H., Jung, Y. B., Cho, M. S., & Tae, S. H. (2015). Effect of supplementary cementitious materials on reduction of CO₂ emissions from concrete. *Journal of Cleaner Production*, 103, 774–783. <https://doi.org/10.1016/j.jclepro.2014.03.018>.
- Yeh, I. C. (2007). Computer-aided design for optimum concrete mixtures. *Cement & Concrete Composites*, 29, 193–202. <https://doi.org/10.1016/j.cemconcomp.2006.11.001>.
- Yepes, V., Martí, J. V., & García-Segura, T. (2015). Cost and CO₂ emission optimization of precast–prestressed concrete U-beam road bridges by a hybrid glowworm swarm algorithm. *Automation in Construction*, 49, 123–134. <https://doi.org/10.1016/j.autcon.2014.10.013>.
- Zhang, Y. R., Zhang, J. Z., Luo, W., Wang, J. D., Shi, J. L., Zhuang, H. X., et al. (2019). Effect of compressive strength and chloride diffusion on life cycle CO₂ assessment of concrete containing supplementary cementitious materials. *Journal of Cleaner Production*, 218, 450–458. <https://doi.org/10.1016/j.jclepro.2019.01.335>.

Publisher's Note

Springer Nature remains neutral with regard to jurisdictional claims in published maps and institutional affiliations.

Submit your manuscript to a SpringerOpen® journal and benefit from:

- Convenient online submission
- Rigorous peer review
- Open access: articles freely available online
- High visibility within the field
- Retaining the copyright to your article

Submit your next manuscript at ► [springeropen.com](https://www.springeropen.com)
